OXFORD

Oxford Open Materials Science, 2023, **3(1),** itad021

https://doi.org/10.1093/oxfmat/itad021
Advance Access Publication Date: 22 November 2023
Research article

Is electrostrain >1% in oxygen deficient $Na_{0.5}Bi_{0.5}TiO_3$ a composition effect?

Getaw Abebe Tina[1], Gudeta Jafo Muleta[1], Gobinda Das Adhikary[1] and Rajeev Ranjan [1,*]

[1]Department of Materials Engineering, Indian Institute of Science, Bangalore 560012, Karnataka, India

*Correspondence address: Department of Materials Engineering, Indian Institute of Science, Bangalore 560012, Karnataka, India. E-mail: rajeev@iisc.ac.in

Abstract

For over two decades $Na_{0.5}Bi_{0.5}TiO_3$ (NBT) -based lead-free piezoelectrics have attracted attention due to its ability to exhibit large electric-field driven strain. Compared to the popular Pb(Zr, Ti)O_3 (PZT)-based piezoelectrics, which exhibit electrostrain of about 0.3%, the derivatives of NBT-based lead-free piezoelectrics at the ergodic—non ergodic relaxor crossover exhibit larger electric-field driven strain ∼0.45%. In recent years, there has been a concerted effort to increase the maximum electrostrain in lead-free piezoceramics. Recent reports suggest that oxygen deficient NBT- based piezoceramics can exhibit electrostrain ∼1%. In this paper we explore this phenomenon and show that the ultra high electric field driven strain measured is primarily a consequence of reducing the thickness of the disc dimension below 500 microns and not an exclusive effect of the composition.

Keywords: piezoelectrics; ferroelectrics; Pb-free piezoceramics; perovskites; $Na_{0.5}Bi_{0.5}TiO_3$; ultrahigh electrostrain

Introduction

For over six decades, the relaxor ferroelectric compound $Na_{0.5}Bi_{0.5}TiO_3$ and its derivatives have attracted considerable attention both from the scientific and technological viewpoints [1–3]. Though discovered almost six decades ago [4] as a rhombohedral ferroelectric compound, the structure and the properties of NBT have puzzled the scientific community for a long time. The structural complexity of NBT owe its origin to the random distribution of Na and Bi on the A-site of the ABO_3 perovskite structure and qualitatively very different character of the Bi-O (covalent) and Na-O (ionic) bonds [5–8]. The local structural disorder in NBT manifests has been explained variedly as deviation of the A-site cation displacements away from the [111] rhombohedral direction [9–11], and to the persistence of the high temperature non-ferroelectric tetragonal (P4/mbm) distortions on the local scale at room temperature [12]. Electron diffraction studies have revealed the presence of short-ranged regions comprising of in-phase ($a^0a^0c^+$) octahedral tilt (characteristic of the P4/mbm distortion) embedded between the relatively long range ordered rhombohedral regions comprising of the $a^-a^-a^-$ type antiphase octahedral tilt [13]. A complex interaction of the two tilt types [14] leads to the global structure (as observed by x-ray diffraction studies) of NBT appear as monoclinic (Cc) [15, 16]. Strong electric field irreversibly transforms the Cc average structure to R3c [17–19]. On the local scale this process is accompanied by irreversible suppression of the in-phase tilted octahedral region [5]. From the property viewpoint this transformation is a field-driven transformation of the non-ergodic relaxor state of NBT to a normal ferroelectric state [5].

The onset of the in-phase octahedral tilt characteristic of the non-polar P4/mbm phase appears on heating NBT above 150°C. This temperature coincides with the onset of the depolarization of poled NBT [5, 18]. Though the system retains the memory of the poling field up to 300°C, the piezoelectric coefficient of poled NBT is drastically reduced when heated to 200°C. This temperature is generally referred to as the depolarization temperature of NBT. NBT-BT [19–27] and NBT-KBT [28–40] are two of the most important NBT solid solution systems as they exhibit morphotropic phase boundary (MPB) in their respective composition-temperature phase diagrams and show enhanced electromechanical responses. However, in comparison to normal ferroelectric based MPB systems like PZT or $BaTiO_3$-based systems, the MPB compositions of NBT-KBT and NBT-BT exhibits a peculiar behavior in the sense that the depolarization temperature exhibits a minimum at the MPB of the later two systems [19]. The dramatic reduction in the depolarization temperature at the MPB of the two NBT-based MPB systems is caused by increased propensity for the in-phase octahedral tilt as the MPB is approached, causing increased structural-polar disorder [19, 41].

The depolarization temperature of NBT-based piezoelectrics is representative of nonergodic—ergodic transformation. In 2007 Zhang *et al.* reported that when certain compositions of NBT-BT is further modified with $K_{0.5}Na_{0.5}NbO_3$ (KNN), the depolarization is further reduced, and that a composition at the crossover of the nonergodic- ergodic relaxor boundary exhibits electrostrain ∼0.5% [42]. Given that the maximum electrostrain obtained from PZT-based polycrystalline piezoelectrics is ∼0.3%, this was considered as an important breakthrough [42]. Since then, attempts have been made to improve the electrostrain of NBT-based systems. Liu and Tan reported electrostrain ∼0.7% in a non-stoichiometric NBT-based system [43].

Recently Luo *et al.* reported that the introduction of oxygen defects in NBT-based piezoceramics simultaneously improved

Received: September 6, 2023. **Revised:** November 1, 2023. **Accepted:** November 11, 2023

the piezoelectric response and the thermal depolarization temperature [44]. The approach involved forming solid solutions of NBT-BT with defect perovskites like $BaAlO_{2.5}$, $BaGaO_{2.5}$ and $BaInO_{2.5}$ to increase the overall tolerance factor of the system alongside the formation of oxygen vacancies [45]. The authors argued that oxygen vacancies increased the tetragonality (c/a) of the system and thereby the depolarization temperature. The role of defect dipoles in enhancing electrostrain in ferroelectrics has been emphasized for quite some time now [46–48]. It has been suggested that compositional design strategies which promote reversible polarization rotation and defect -induced pinning effect can also help in improving the high field electrostrain values [45]. A strain of 1.1% at 100 kV/cm was recently reported for a composition 0.94NBT- $0.06BaAlO_{2.5}$. Prior to the strain measurement, the specimen was aged in a dc field. The authors argued that aging the specimen under DC field oriented the defect dipoles along a preferable direction. It provided the restoring force for large reversible switching of the domains. The strain ∼1.1% in 0.94NBT- $0.06BaAlO_{2.5}$ is almost similar to the strain of ∼1.3% at 80 kV/cm, reported earlier by Narayan *et al.* in La modified $BiFeO_3$-$PbTiO_3$ (BF-PT) [49]. However, it is important to note that no aging was required to obtain large strain in the La modified BF-PT [49]. Given that (1-x)NBT-(x)BT exhibits MPB at x ∼ 0.06, it is anticipated that the electrostrain can be further enhanced by introducing oxygen defects of the NBT -based MPB systems. Interesting to note that no such large strain values were reported by Luo *et al.* in the (1-y)[(1-x)$Na_{0.5}Bi_{0.5}TiO_3$-(x)$BaTiO_3$] -y$BaAlO_{2.5}$ (NBT-BT-BAO) [44]. The bipolar strain of this pseudo ternary system is reported to be significantly lower (in the range 0.2–0.25%) than the ∼1% strain reported for (1-y)$Na_{0.5}Bi_{0.5}TiO_3$-y$BaAlO_{2.5}$ [45]. This is quite puzzling and suggests that something is missing in our understanding of what drives large electrostrain in these systems. In this paper we have investigated this issue in detail and found that it is not the composition which is responsible for the large electrostrain value but the dimension of the ceramic disc. We succeeded in obtaining large electrostrain values (>2%) even in the $BaAlO_{2.5}$ modified MPB composition 0.935NBT-0.065BT. Our study sheds new light on the phenomenon of large electrostrain in piezoceramics

Experimental methods

Lead-free polycrystalline (1-x)(0.935$Na_{1/2}Bi_{1/2}TiO_3$-0.065$BaTiO_3$)-(x)$BaAlO_{2.5}$ (where x = 0.00, 0.01, 0.03, 0.05 and 0.07 mol) piezoceramics were prepared by conventional solid-state reaction method using dried Al_2O_3 (99.9%, Alfa Aesar), $BaCO_3$ (99.8%, Alfa Aesar), Bi_2O_3 (99%, Alfa Aesar), Na_2CO_3 (99.8% Alfa Aesar), and TiO_3 (99.8%, Alfa Aesar) as raw materials. The designed composition of raw oxides were weighed and then ball milled in a planetary ball mill with acetone medium for 12 h. The resulting mixture were dried and calcined in alumina crucible at 900°C for 3 h. Afterward, the calcined powders were subjected to another round of ball milled for 8 h, mixed with 5% PVA, and pressed into disk green pellets at 100 MPa by unidirectional pressing followed by cold isostatic pressed at 300 MPa. The green pellets were sintered in a muffle furnace at 1160°C for 3 h inside cup-cone alumina crucibles to minimize the loss of Na and Bi atoms, then sintered pellets were polished and coated with silver electrodes on both sides of the surface for electrical characterization. The pellets were poled at 60 kV/cm dc source in non-conductive silicone oil media for 20 min using IATOME, India, and then measured direct piezoelectric response (d_{33}) on poled pellets using Piezotest (PM300) with the frequency 110 Hz and applied force 0.25 N. Both unpoled and poled X-ray powder diffraction (XRPD) of specimens were carried out using a Cu-Ka1 X-Ray Diffractometer (Rigaku, Smart lab). The morphology and grain size distribution of specimens were studied by using a Scanning electron microscope (FESEM, Zeiss). The density of sintered pellets measured by Archimedes liquid displacement method was ∼95% dense (Supplementary Fig. S1 and Table S1). Ferroelectric (P-E) hysteresis loops and electrostrain (S-E) curves were recorded using a ferroelectric workstation (Radiant Technologies Inc) in insulating silicon medium by applied ac field of 70 to 80 kV/cm having a frequency of 1 Hz at room temperature.

Results and discussion

Here we have focused on the MPB composition 0.935NBT-0.065BT of the NBT-BT series and modified it with $BaAlO_{2.5}$ as per the nominal chemical formula (1-x)(0.935$Na_{1/2}Bi_{1/2}TiO_3$-

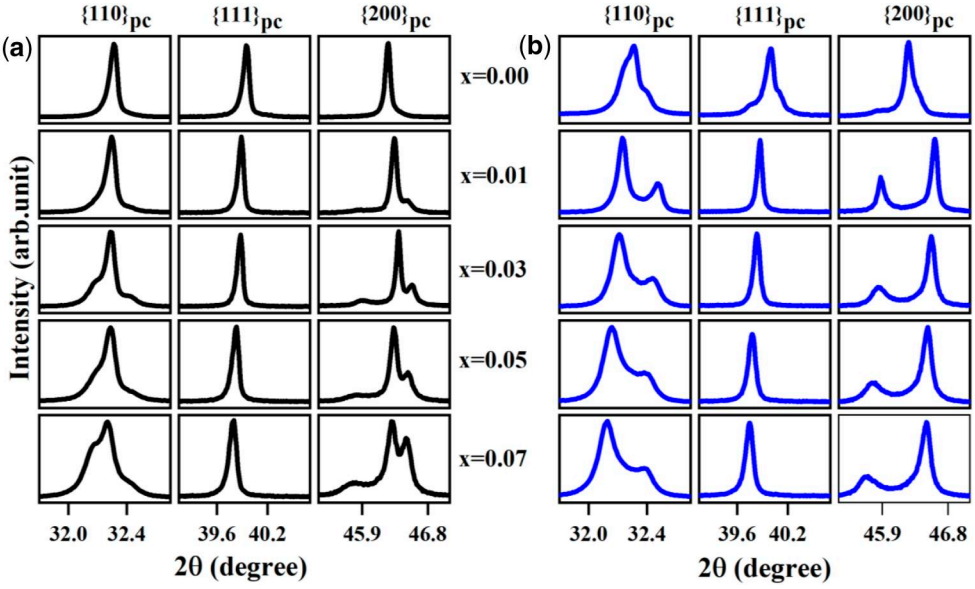

Figure 1. Composition evolution of the selected pseudocubic (pc) X-ray powder diffraction Bragg profiles of $\{110\}_{pc}$, $\{111\}_{pc}$, and $\{200\}_{pc}$ (**a**) unpoled and (**b**) poled specimens.

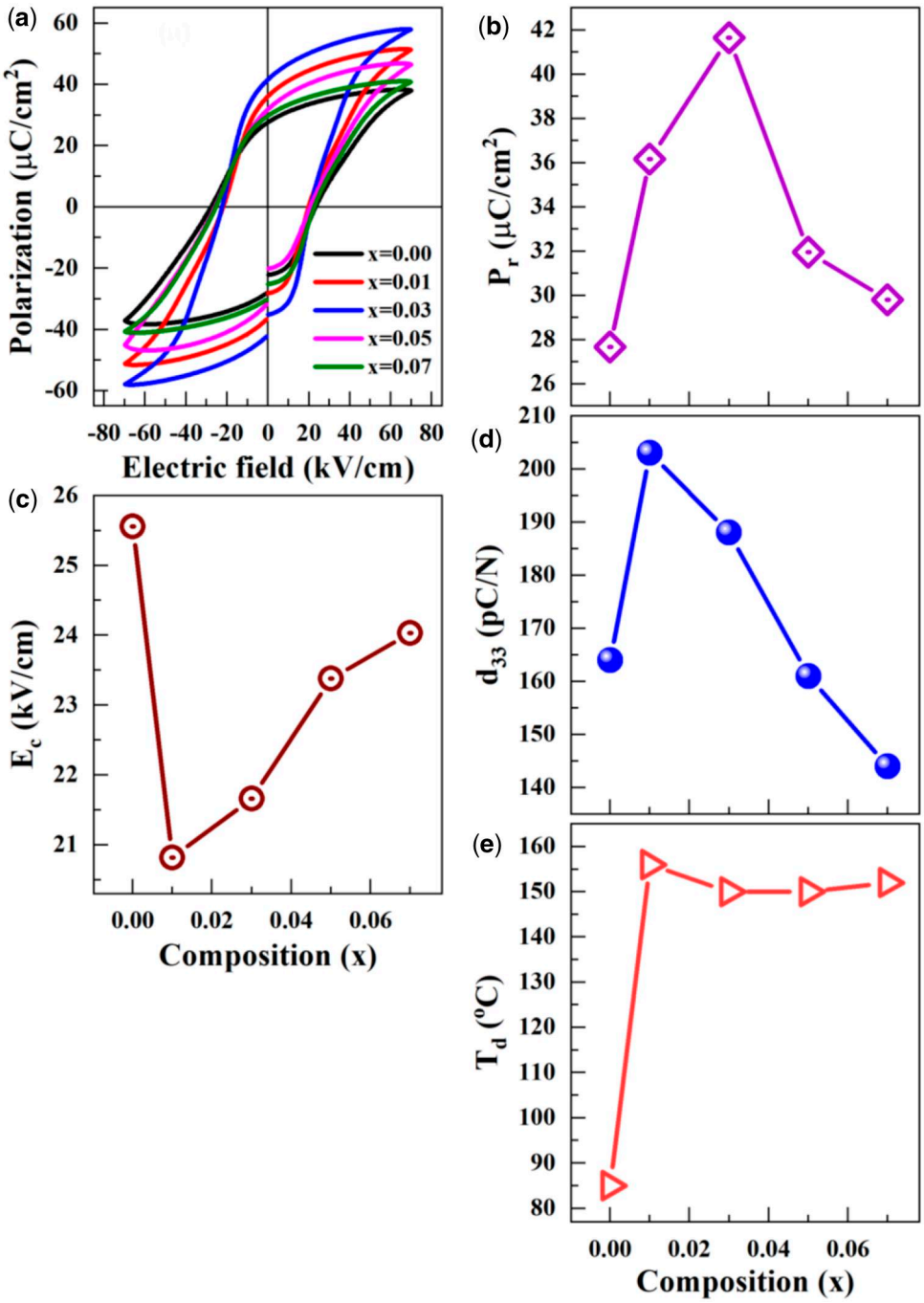

Figure 2. (**a**) Polarization hysteresis (P-E) loops measured at 1 Hz for the (1-x)(0.935$Na_{1/2}Bi_{1/2}TiO_3$-0.065$BaTiO_3$)-(x)$BaAlO_{2.5}$ ceramics. The relative change in (**b**) remnant polarization (P_r), (**c**) coercive field (E_c), (**d**) Longitudinal direct piezoelectric coefficient (d_{33}), and (**e**) depolarization temperature (T_d) values of ceramics as a function of composition x.

0.065$BaTiO_3$)-(x)$BaAlO_{2.5}$. Figure 1a shows the evolution of the $\{110\}_{pc}$, $\{111\}_{pc}$ and $\{200\}_{pc}$ pseudocubic x-ray Bragg profiles of as a function of x. The diffraction patterns were collected after grinding the sintered ceramic discs to powder followed by thermal annealing to 500°C for 2 h to remove the stress effects caused by the grinding process. Consistent with the previous reports [20–22] the singlet nature of all the Bragg profiles suggests a cubic like structure of the unmodified (x = 0.00) MPB composition. With increasing the BAO concentration (x), the $\{110\}_{pc}$ and the $\{200\}_{pc}$ Bragg profiles develop split. This split is indicative of the development of a long-range tetragonal distortion in the system. The increasing intensity of the tetragonal peaks suggests that more volume fraction of the cubic like phase transformed to the long-ranged tetragonal phase with increasing x.

We also collected diffraction patterns from poled specimens of the different compositions. The diffraction patterns of the poled specimens were taken after griding the poled pellets to powder. The random orientation of the powder specimen gives preferred orientation free diffraction pattern while retaining the irreversible changes brought about by the poling field [22, 50]. The diffraction pattern of the poled x = 0.00 shows $\{110\}_{pc}$, $\{111\}_{pc}$ and $\{200\}_{pc}$ as triplets. This confirms that the poling field has irreversibly transformed the cubic like phase to a mixture of long ranged rhombohedral and tetragonal ferroelectric phases,

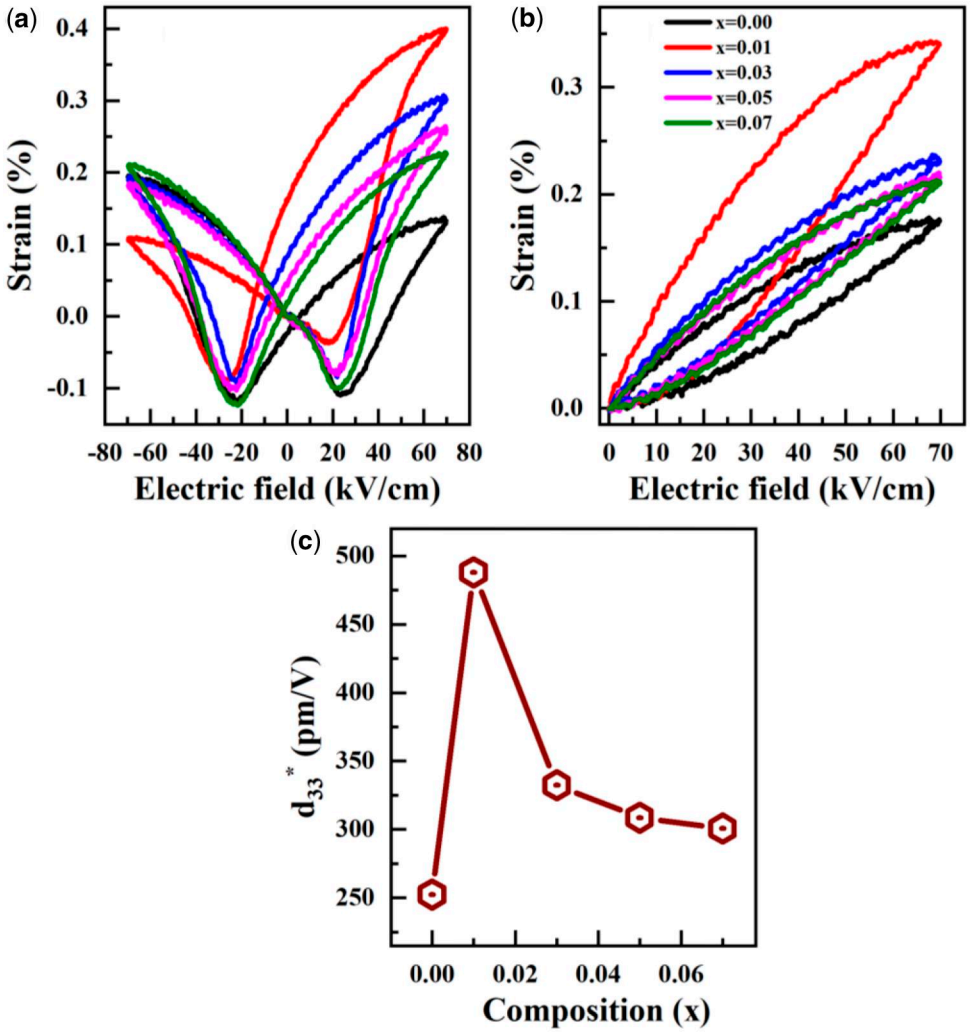

Figure 3. (**a**) Bipolar strain curves and (**b**) unipolar strain curves of the specimens with the electric field, and (**c**) converse piezoelectric coefficient (d_{33}*) of ceramics at an electric field of 70 kV/cm with a function of composition x.

Fig. 1b. The poled BAO modified compositions ($x \geq 0.01$), on the other hand, show only long ranged tetragonal ferroelectric phase.

Figure 2 shows the composition dependence of ferroelectric and piezoelectric properties. All compositions show well-behaved polarization electric field hysteresis loop under bipolar cycling. The remanent polarization increased from 27 μC/cm^2 for $x = 0.00$ to 42 μC/cm^2 up to $x = 0.03$. The longitudinal piezoelectric coefficient, d_{33} from ∼165 pC/N for $x = 0.00$ to a maximum of 205 pC/N for $x = 0.01$. In general, given all other parameters being equal, a specimen with higher polarization is expected to exhibit higher d_{33}. In the present case, the coercive field of $x = 0.01$ is the lowest (Fig. 2c). That is, the domains in $x = 0.01$ are more mobile than in $x = 0.03$. This factor seems to make $x = 0.01$ show relatively better piezoelectric coefficient than $x = 0.03$. Interestingly, the depolarization temperature increased abruptly from 85°C for $x = 0.00$ to 155°C for $x = 0.01$. The abrupt increase of T_d at $x = 0.01$ can be understood from the fact that the average structure of poled $x = 0.00$ is rhombohedral + tetragonal and for $x = 0.01$ is tetragonal. In an MPB piezoelectrics, the tetragonal phase, generally exhibit significantly higher depolarization temperature. Another important point to note is that the d_{33} is maximum for the tetragonal composition at the boundary of the two phase (rhombohedral + tetragonal) region, and not for the composition exhibiting the phase mixture. This observation is similar to what was reported earlier by Adhikary *et al.* for (1-z)NBT-(z)KBT [37]. The phase coexistence region in (1-z)NBT-(z)KBT spans $0.20 < z < 0.25$ and the tetragonal composition $z = 0.25$ exhibit the maximum piezoelectric response [37]. This suggests that the best piezoelectric response in piezoelectric systems exhibiting MPB should be sought in tetragonal composition at the boundary of the two-phase region.

Figure 3 shows the bipolar and unipolar electrostrain of (1-x)(0.935$Na_{1/2}Bi_{1/2}TiO_3$-0.065$BaTiO_3$)-(x)$BaAlO_{2.5}$ at room temperature measured with a triangular wave waveform with field amplitude 70 kV/cm. The butterfly strain loop is evidently asymmetric with more strain in the positive cycle as compared to the negative cycle. The maximum strain (at 70 kV/cm) in the positive cycle is ∼0.4% for $x = 0.01$. The same composition shows strain of 0.1% in the negative cycle. For actuator applications, the unipolar electrostrain is of practical significance. Interestingly, the unipolar electrostrain (measured for the positive cycle) is maximum (∼0.35%) for the same composition ($x = 0.01$) which exhibits maximum d_{33}. This scenario is different from the strategy which emphasizes extracting maximum strain in compositions at the ergodic-non ergodic relaxor boundaries in NBT-based piezoelectrics [42, 43]. Since such compositions cannot be poled, they show nearly zero d_{33}. Important to note that the maximum electrostrain reported by

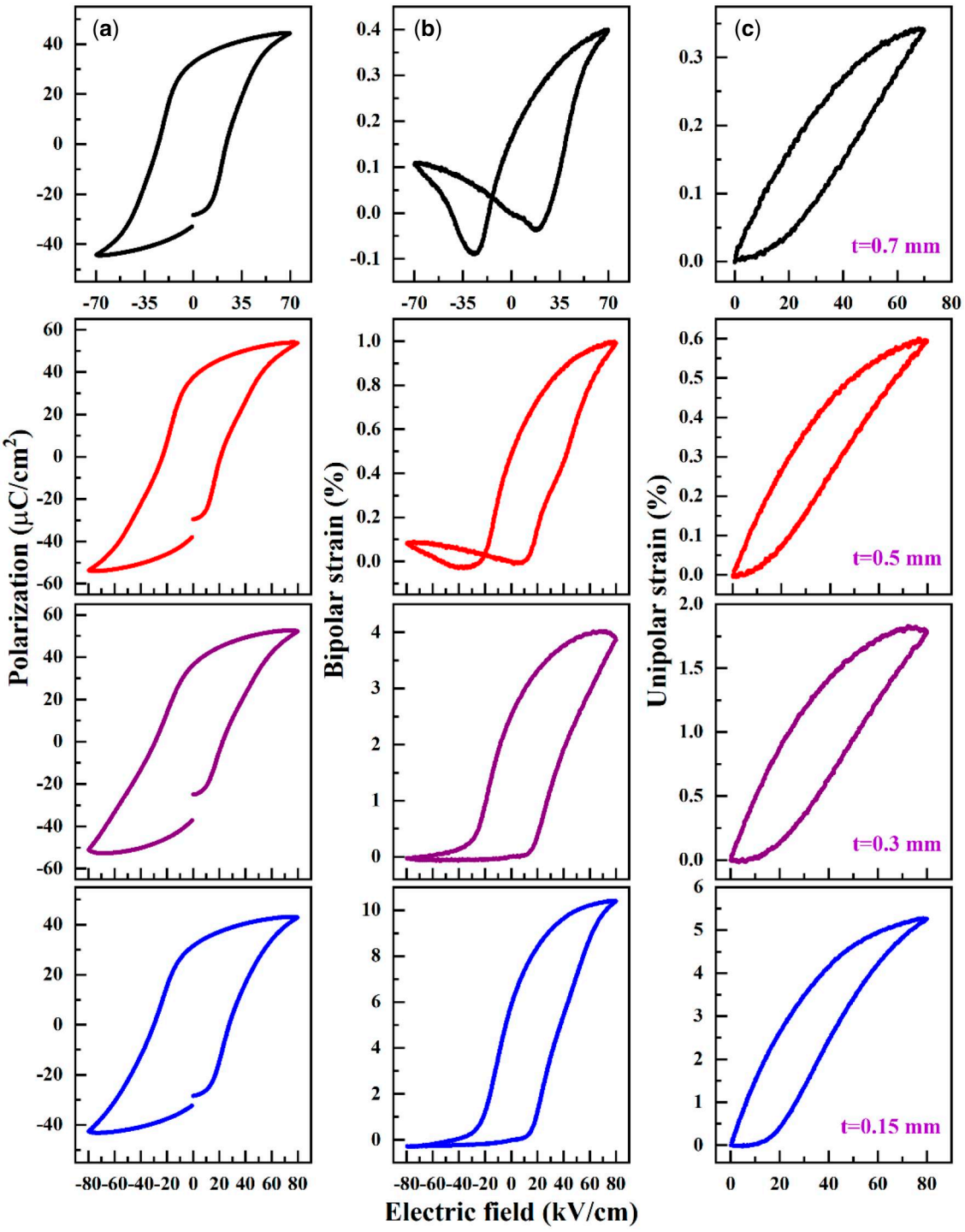

Figure 4. Thickness dependence ferroelectric and piezoelectric measurements of a composition x = 0.01. (**a**) P-E hysteresis loops, (**b**) bipolar S-E curves, and (**c**) unipolar S-E curves for the thickness of 0.7, 0.5, 0.3, and 0.15 mm measured at 1 Hz and room temperature.

Luo *et al.* for (1-y)0.94NBT-0.06BT)-(y)$BaAlO_{2.5}$ with y = 0.05 is in the range 0.2 to 0.25% at similar field values [44]. The authors did not report unipolar strain in their paper. However, it is anticipated to be lower than the strain obtained in bipolar field cycling. At this point we would like to emphasize that the electrostrain measurements performed by us were on circular discs of thickness of diameter ∼10 mm and thicknesses of 0.7 mm. Luo *et al.* measured electrostrain values on thickness disc thickness of 1 mm. In contrast, the electrostrain of 1.12% reported by Luo *et al.* on a non-MPB composition 0.94NBT-0.06$BaAlO_{2.5}$ was measured on ceramic discs of thickness 0.3–04 mm [45]. While it may not seem obvious as to how the thickness of the piezoceramic disc be a factor in determining the electrostrain we measure on the discs, recently Adhikary *et al.* have shown that thickness of the ceramic disc does matter in the electrostrain we measure [51]. Below we show that the same phenomenon is applicable to (1-x)(0.935$Na_{1/2}Bi_{1/2}TiO_3$-0.065$BaTiO_3$)-(x)$BaAlO_{2.5}$.

Figure 4 shows the thickness dependence of the polarization, bipolar and unipolar strain loops of the critical composition

x = 0.01. While the P-E loops are not affected notably on decreasing the disc thickness, the bipolar strain loop becomes increasingly more asymmetric. The strain in the positive cycle are 0.4% for the 0.7 mm, ∼1.0% for 0.5 mm, ∼4% for the 0.3 mm disc and 10% for 0.15 mm disc. The unipolar strain values are 0.35, 0.6, 1.8 and ∼5% for 0.7, 0.5 and 0.3 and 0.15 mm thickness, respectively. The effect of reducing the thickness down to 0.2mm for other compositions (x = 0.03, 0.05 and 0.08) can be found in Supplementary Figs S2 and S3. Such highly asymmetric bipolar strain has earlier been referred to as hetrostrain [52] and caused by oxygen defects. We show here that it is rather a phenomenon of thickness reduction. In fact, for similar composition as ours, Luo *et al.* reported very low strain ∼0.2% at 80 kV/cm in oxygen deficient MPB compositions of [(1-y](1-x)NBT-(x)$BaTiO_3$-(y)$BaAlO_{2.5}$ [44]. The large value of strain ∼1% was reported for a non MPB composition x = 0.00 [45]. In view of our results, this apparent contradiction in the two papers of Luo *et al.* [44, 45] can be understood by because the two works were carried out on ceramic discs with distinctly different thicknesses. While the study reporting lower (∼0.2%) electrostrain used 1 mm thick ceramic discs, the one reporting strain of 1.12% strain used discs ∼0.3 mm. As our study has clearly shown, the electrostrain decreases sharply below on increasing the disc thickness. For 0.7 mm thickness, we obtain strain of 0.4%. It is therefore no surprise that the 1 mm thick discs show strain of ∼0.2%.

In summary, our work has shown that large electrostrain in oxygen deficient [(1-y](1-x)NBT-(x)$BaTiO_3$-(y)$BaAlO_{2.5}$ reported recently is not a composition effect. We have shown that compositions close to the morphotropic phase boundary of this system can exhibit electrostrain >1% only if the thickness of the ceramic discs is kept low (<0.5 mm). Large electrostrain is therefore primarily a thickness effect. Although at present there is no clear understanding of the mechanism underlying this intriguing phenomenon, it is important to report the phenomenon *per se* to make the scientific community aware about it. The bipolar strain reaching 10% value in 0.15 mm thick disc of our specimen is extraordinary. In this context it is worth highlighting the possibility of the large strain being measured because of bending of the ceramic discs. He *et al.* [53] has recently reported a nominal strain of 0.7% at 150 kV/cm in a non-perovskite piezoceramic Bi_2WO_6. The authors reported highly asymmetric bipolar strain, similar to what we have shown above, and argued the possibility of the disc bending due to asymmetric 90-degree ferroelastic switching in the upper and lower surfaces of the disc.

Supplementary data

Supplementary data is available at *Oxford Open Immunology Journal* online.

Data availability

The relevant data are available in the paper.

Authors' contributions

Getaw Abebe Tina (Data curation [equal], Formal analysis [equal], Investigation [equal], Writing—original draft [equal]), Gudeta Jafo Muleta (Data curation [equal], Formal analysis [equal], Investigation [equal]), Gobinda Das Adhikary (Conceptualization [equal], Data curation [equal], Formal analysis [equal], Investigation [equal], Methodology [equal], Supervision [equal]), and Rajeev Ranjan (Conceptualization [equal], Formal analysis [equal], Funding acquisition [equal], Investigation [equal], Methodology [equal], Project administration [equal], Supervision [equal], Writing—review & editing [equal])

Conflict of interest statement: The authors declare no conflict of interest.

Funding

R.R. is grateful to the Science and Engineering Research Board (SERB) India for supporting this work (Grant no. CRG/2021/000134).

References

1. Ranjan R. $Na_{1/2}Bi_{1/2}TiO_3$-based lead-free piezoceramics: A review of structure property correlation. *Current Science* 2020; **118**:1507.
2. Rödel J, Webber KG, Dittmer R *et al.* Transferring lead-free piezoelectric ceramics into application. *J Eur Ceram Soc* 2015; **35**:1659–81.
3. Paterson AR, Nagata H, Tan X *et al.* Relaxor-ferroelectric transitions: Sodium bismuth titanate derivatives. *MRS Bull* 2018; **43**:600–6.
4. Smolensky GA, Isupov VA, Agranovskaya AI *et al.* New materials of $A_2B_2O_6$ type. *Trans Sov Phys Solid State* 1961;**2**:2651.
5. Rao BN, Datta R, Chandrashekaran SS *et al.* Local structural disorder and its influence on the average global structure and polar properties in $Na_{0.5}Bi_{0.5}TiO_3$. *Phys Rev B* 2013;**88**:224103.
6. Shuvaeva VA, Zekria D, Glazer AM *et al.* Local structure of the lead-free relaxor ferroelectric $(KxNa_{1-x})_{0.5}Bi_{0.5}TiO_3$. *Phys Rev B* 2005;**71**:174114.
7. Rao BN, Olivi L, Sathe V *et al.* Electric field and temperature dependence of the local structural disorder in the lead-free ferroelectric $Na_{0.5}Bi_{0.5}TiO_3$: An EXAFS study. *Phys Rev B* 2016; **93**:024106.
8. Usher TM, Levin I, Daniels JE *et al.* Electric field- induced local and mesoscale structural changes in polycrystalline dielectrics and ferroelectrics. *Sci Rep* 2015;**5**:14678.
9. Thomas PA, Trujillo S, Boudard M *et al.* Diffuse X-ray scattering in the lead-free piezoelectric crystals $Na_{1/2}Bi_{1/2}TiO_3$ and Ba-doped $Na_{1/2}Bi_{1/2}TiO_3$. *Solid State Sci* 2010;**12**:311–7.
10. Kreisel J, Bouvier P, Dkhil B *et al.* High-pressure X-ray scattering of oxides with a nanoscale local structure: Application to $Na_{1/2}Bi_{1/2}TiO_3$. *Phys Rev B* 2003;**68**:014113.
11. Matsuura M, Iida H, Hirota K *et al.* Damped soft phonons and diffuse scattering in $(Bi_{1/2}Na_{1/2})TiO_3$. *Phys Rev B* 2013;**87**:064109.
12. Balagurov AM, Koroleva EY, Naberezhnov AA *et al.* The rhombohedral phase with incommensurate modulation in $Na_{1/2}Bi_{1/2}TiO_3$. *Phase Transit* 2006;**79**:163–73.
13. Dorcet V, Trolliard G. A transmission electron microscopy study of the A-site disordered perovskite $Na_{0.5}Bi_{0.5}TiO_3$. *Acta Mater* 2008;**56**:1753–61.
14. Levin I, Reaney IM. Nano- and mesoscale structure of $Na_{1/2}Bi_{1/2}TiO_3$: A TEM perspective. *Adv Funct Materials* 2012; **22**:3445–52.
15. Gorfman S, Thomas PA. Evidence for a nonrhombohedral average structure in the lead-free piezoelectric material $Na_{0.5}Bi_{0.5}TiO_3$. *J Appl Crystallogr* 2010;**43**:1409–14.
16. Aksel E, Forrester JS, Jones JL *et al.* Monoclinic crystal structure of polycrystalline $Na_{0.5}Bi_{0.5}TiO_3$. *Appl. Phys. Lett* 2011;**98**:152901.

17. Rao BN, Ranjan R. Electric-field-driven monoclinic-to rhombohedral transformation in $Na_{1/2}Bi_{1/2}TiO_3$. *Phys Rev B* 2012; **86**:134103.
18. Rao BN, Fitch AN, Ranjan R. Ferroelectric- ferroelectric phase coexistence in $Na_{1/2}Bi_{1/2}TiO_3$. *Phys Rev B* 2013;**87**:060102.
19. Adhikary GD, Mahale B, Rao BN *et al.* Depoling phenomena in $Na_{0.5}Bi_{0.5}TiO_3$-$BaTiO_3$: A structural perspective. *Phys Rev B* 2021; **103**:184106.
20. Ranjan R, Dviwedi A. Structure and dielectric properties of $(Na_{0.5}Bi_{0.5})_{1-x}BaxTiO_3$: $0 \leq x \leq 0.10$. *Solid State Commun* 2005; **135**:394–9.
21. Jo W, Daniels JE, Jones JL *et al.* Evolving morphotropic phase boundary in lead-free $(Bi_{1/2}Na_{1/2})TiO_3$–$BaTiO_3$ piezoceramics. *J. Appl. Phys* 2011;**109**:014110.
22. Garg R, Narayana Rao B, Senyshyn A *et al.* Long ranged structural modulation in the pre-morphotropic phase boundary cubic-like state of the lead-free piezoelectric $Na_{1/2}Bi_{1/2}TiO_3$–$BaTiO_3$. *J. Appl. Phys* 2013;**114**:234102.
23. Ma C, Guo H, Tan X. A new phase boundary in $(Bi_{1/2}Na_{1/2})TiO_3$–$BaTiO_3$ revealed via a novel method of electron diffraction analysis. *Adv Funct Materials* 2013;**23**:5261–6.
24. Ma C, Guo H, Beckman SP, Tan X. Creation and destruction of morphotropic phase boundaries through electrical poling: A case study of lead-free $(Bi_{1/2}Na_{1/2})TiO_3$–$BaTiO_3$ piezoelectrics. *Phys Rev Lett* 2012;**109**:107602.
25. Khatua DK, Mishra A, Kumar N *et al.* A coupled microstructural structural mechanism governing thermal depolarization delay in $Na_{0.5}Bi_{0.5}TiO_3$-based piezoelectrics. *Acta Mater* 2019; **179**:49–60.
26. Jo W, Daniels J, Damjanovic D *et al.* Two-stage processes of electrically induced-ferroelectric to relaxor transition in $0.94(Bi_{1/2}Na_{1/2})TiO_3$–$0.06BaTiO_3$. *Appl. Phys. Lett* 2013;**102**:192903.
27. Khatua DK, Kalaskar A, Ranjan R. Tuning photoluminescence response by electric field in electrically soft ferroelectrics. *Phys Rev Lett* 2016;**116**:117601.
28. Pronin IP, Parfenova NN, Zaitseva NV *et al.* Phase transitions in solid solutions of sodium bismuth and potassium bismuth titanates. *Sov. Phys. Solid State* 1982;**24**:1060–2.
29. Sasaki A, Chiba T, Mamiya Y *et al.* Dielectric and piezoelectric properties of $(Bi_{0.5}Na_{0.5})TiO_3$–$(Bi_{0.5}K_{0.5})TiO_3$ systems. *Jpn J Appl Phys* 1999;**38**:5564.
30. Otoničar M, Škapin SD, Spreitzer M *et al.* Compositional range and electrical properties of the morphotropic phase boundary in the $Na_{0.5}Bi_{0.5}TiO_3$–$K_{0.5}Bi_{0.5}TiO_3$ system. *J. Eur. Ceram. Soc* 2010; **30**:971–9.
31. Jones GO, Kreisel J, Thomas PA. A structural study of the $(Na_{1-x}Kx)_{0.5}Bi_{0.5}TiO_3$ perovskite series as a function of substitution (*x*) and temperature. *Powder Diffr* 2002;**17**:301–19.
32. Levin I, Reaney IM, Anton E-M *et al.* Local structure, pseudosymmetry, and phase transitions in $Na_{1/2}Bi_{1/2}TiO_3$–$K_{1/2}Bi_{1/2}TiO_3$ ceramics. *Phys Rev B* 2013;**87**:024113.
33. Goetzee-Barral AJ, Usher TM, Stevenson TJ *et al.* Electric field dependent local structure of $(KxNa_{1-x})_{0.5}Bi_{0.5}TiO_3$. *Phys Rev B* 2017; **96**:014118.
34. Zhang S, Shrout TR, Nagata H *et al.* Piezoelectric properties in $(K_{0.5}Bi_{0.5})TiO_3$–$(Na_{0.5}Bi_{0.5})TiO_3$–$BaTiO_3$ lead-free ceramics. *IEEE Trans Ultrason, Ferroelect, Freq Contr* 2007;**54**:910–7.
35. Elkechai O, Manier M, Mercurio JP. $Na_{0.5}Bi_{0.5}TiO_3$–$K_{0.5}Bi_{0.5}TiO_3$ (NBT–KBT) system: A structural and electrical study. *Phys Stat Sol (a)* 1996;**157**:499–506.
36. Babu MVG, Bagyalakshmi B, Venkidu L *et al.* Grain size effect on structure and electrical properties of lead-free $Na_{0.4}K_{0.1}Bi_{0.5}TiO_3$ ceramics. *Ceram. Int* 2017;**43**:12599–604.
37. Adhikary GD, Dwij V, Senyshyn A *et al.* Large nonlinear electrostrain and piezoelectric response in nonergodic $(Na, K)_{0.5}Bi_{0.5}TiO_3$: Synergy of structural disorder and tetragonal phase in proximity to a morphotropic phase boundary. *Phys Rev Mater* 2021;**5**:064414.
38. Adhikary GD, Muleta GJ, Tina GA *et al.* Structural insights into electric field induced polarization and strain responses in K0.5Na0.5NbO3 modified morphotropic phase boundary compositions of Na0.5Bi0.5TiO3-based lead-free piezoelectrics. *Phys Rev B* 2023;**107**:134108.
39. Adhikary GD, Mahale B, Senyshyn A *et al.* Relaxor ground state forced by ferroelastic instability in $K_{0.5}Bi_{0.5}TiO_3$-$Na_{0.5}Bi_{0.5}TiO_3$. *Phys Rev B* 2020;**102**:184113.
40. Adhikary GD, Khatua DK, Senyshyn A *et al.* Random lattice strain and its relaxation towards the morphotropic phase boundary of $Na_{0.5}Bi_{0.5}TiO_3$-based piezoelectrics: Impact on the structural and ferroelectric properties. *Phys Rev B* 2019; **99**:174112.
41. Adhikary GD, Khatua DK, Mishra A *et al.* Increasing intervention of nonferroelectric distortion and weakening of ferroelectricity at the morphotropic phase boundary in $Na_{0.5}Bi_{0.5}TiO_3$-$BaTiO_3$. *Phys Rev B* 2019;**100**:134111.
42. Zhang S-T, Kounga AB, Aulbach E *et al.* Giant strain in lead-free piezoceramics $Bi_{0.5}Na_{0.5}TiO_3$–$BaTiO_3$–$K_{0.5}Na_{0.5}NbO_3$ system. *Appl Phys Lett* 2007;**91**:112906.
43. Li T, Lou X, Ke X *et al.* Giant strain with low hysteresis in A-site-deficient$(Bi_{0.5}Na_{0.5})TiO_3$-based lead-free piezoceramics. *Acta Mater* 2017;**128**:337–44.
44. Luo H, Liu H, Deng S *et al.* Simultaneously enhancing piezoelectric performance and thermal depolarization in lead-free (Bi, Na)TiO_3-$BaTiO_3$ via introducing oxygen-defect perovskites. *Acta Mater* 2021;**208**:116711.
45. Luo H, Liu H, Huang H *et al.* Achieving giant electrostrain of above 1% in (Bi,Na)TiO_3-based lead-free piezoelectrics via introducing oxygen-defect composition. *Sci Adv* 2023;**9**:7078.
46. Ren X. Large electric-field-induced strain in ferroelectric crystals by point defect mediated reversible domain switching. *Nature Mater* 2004;**3**:91–4.
47. Kimmel AV, Weaver PM, Cain MG *et al.* Defect-mediated lattice relaxation and domain stability in ferroelectric oxides. *Phys Rev Lett* 2012;**109**:117601.
48. Erhart P, Träskelin P, Albe K. Formation and switching of defect dipoles in acceptor doped lead titanate: A kinetic model based on first-principles calculations. *Phys Rev B* 2013;**88**:024107.
49. Narayan B, Malhotra JS, Pandey R *et al.* Electrostrain in excess of 1% in polycrystalline piezoelectrics. *Nature Mater* 2018; **17**:427–31.
50. Lalitha KV, Kalyani AK, Ranjan R. Analogous stress and electric field driven structural transformation and decrease in polarization coherence on poling around the morphotropic phase boundary in $BiScO_3$-$PbTiO_3$. *Phys Rev B* 2014;**90**:224107.
51. Adhikary GA, Singh DN, Tina GA *et al.* Ultrahigh electrostrain >1% in lead-free piezoceramics: Role of disk dimension. *J Appl Phys* 2023;**134**:054101.
52. Feng W, Luo B, Bian S *et al.* Heterostrain-enabled ultrahigh electrostrain in lead-free piezoelectric. *Nat Commun* 2022;**13**:5086.
53. He X, Chen C, Wang L *et al.* Giant electromechanical response in layered ferroelectrics enabled by asymmetric ferroelastic switching. *Mater Today* 2022;**58**:48–56.